

The Ribosome Restrains Molten Globule Formation in Stalled Nascent Flavodoxin*

Received for publication, August 30, 2016, and in revised form, October 13, 2016. Published, JBC Papers in Press, October 26, 2016, DOI 10.1074/jbc.M116.756205

Joseline A. Houwman, Estelle André, Adrie H. Westphal, Willem J. H. van Berkel, and Carlo P. M. van Mierlo¹

From the Laboratory of Biochemistry, Wageningen University, 6708 WE Wageningen, The Netherlands

Edited by Linda Spremulli

Folding of proteins usually involves intermediates, of which an important type is the molten globule (MG). MGs are ensembles of interconverting conformers that contain (non-)native secondary structure and lack the tightly packed tertiary structure of natively folded globular proteins. Whereas MGs of various purified proteins have been probed to date, no data are available on their presence and/or effect during protein synthesis. To study whether MGs arise during translation, we use ribosome-nascent chain (RNC) complexes of the electron transfer protein flavodoxin. Full-length isolated flavodoxin, which contains a non-covalently bound flavin mononucleotide (FMN) as cofactor, acquires its native α/β parallel topology via a folding mechanism that contains an off-pathway intermediate with molten globular characteristics. Extensive population of this MG state occurs at physiological ionic strength for apoflavodoxin variant F44Y, in which a phenylalanine at position 44 is changed to a tyrosine. Here, we show for the first time that ascertaining the binding rate of FMN as a function of ionic strength can be used as a tool to determine the presence of the off-pathway MG on the ribosome. Application of this methodology to F44Y apoflavodoxin RNCs shows that at physiological ionic strength the ribosome influences formation of the off-pathway MG and forces the nascent chain toward the native state.

Proteins need to fold into their correct native conformations to perform their functions. Folding progresses from unfolded to natively folded protein and often involves intermediates (1, 2). Some of these intermediates are dead ends within the folding funnel (*i.e.* local minima in free energy) and must therefore (partially) unfold before the productive folding pathway can be followed (3). Molten globules are a specific type of folding intermediates, which contain secondary structure elements but lack the tight tertiary packing found in natively folded proteins. Molten globular intermediates can reside on or off the folding pathway to native protein. MGs² are prone to aggregation and consequently are implicated in various diseases (4).

Since the first description of MGs (5), much research has focused on determining conditions at which MGs form. Several proteins form these intermediates under mildly alkaline or acidic conditions (6–9). Currently, many proteins are thought to fold via MG intermediates (10–13). For example, it has been postulated that the occurrence of MG species is necessary during insertion of proteins into membranes or through membrane pores (14–16). Such insertions often happen co-translationally, *i.e.* while the ribosome synthesizes the protein concerned. It has been shown that proteins can fold co-translationally and sample intermediate folding states (17–23), which might include MGs.

Determining the ability of the proteins to form co-translational MGs would be a stepping-stone in elucidating protein folding in the cell, and potentially, it contributes to understanding the initiation of protein aggregation. Characterization of MGs is complicated by their often transient nature, generally low presence at equilibrium, conformational heterogeneity, and the tendency to aggregate (24). The presence of MGs can be revealed through use of extrinsic dyes, such as thioflavin T (ThT), as these dyes become highly fluorescent upon binding to exposed hydrophobic residues (25). Other methods for MG detection include circular dichroism and intrinsic tryptophan fluorescence (26–28). However, these methodologies are unsuitable for studying co-translational MG formation, as ribosome-nascent chain complexes (RNCs) not only contain the emerging polypeptide but also more than 50 ribosomal proteins. Thus, detection of MG formation on the ribosome is notoriously difficult.

To investigate whether nascent chains form MGs, we utilize a 179-residue flavodoxin from *Azotobacter vinelandii*. Flavodoxin contains a non-covalently bound flavin mononucleotide (FMN) as cofactor and is involved in electron transport in the nitrate reduction cycle. The native protein consists of five α -helices sandwiching a central parallel β -sheet, which is an α/β parallel topology (Fig. 1, *left*) (29). According to Structural Classification of Proteins in the Protein Data Bank, approximately 25% of proteins share this topology. The flavodoxin-like fold is an ancestral fold (30) and is archetypal for the class of $\alpha\beta\alpha$ sandwiches. It has been well established that proteins with a flavodoxin-like architecture fold *in vitro* through involvement of an off-pathway intermediate (11, 31–37). Upon folding, the large majority of unfolded flavodoxin molecules temporarily misfold. This misfolding yields an off-pathway MG that is prone to aggregation (38). In contrast to native protein, this MG contains no β -sheet and is helical (Fig. 1, *middle*) (33, 39, 40).

* This work was supported by ECHO Grant 711.011.007 from Netherlands Organisation for Scientific Research (NWO) (to C. P. M. v. M.). The authors declare that they have no conflicts of interest with the contents of this article.

✎ Author's Choice—Final version free via Creative Commons CC-BY license.

¹ To whom correspondence should be addressed: Laboratory of Biochemistry, Wageningen University, Stippeneng 4, 6708 WE Wageningen, The Netherlands. Tel.: 31-317-484621; E-mail: carlo.vanmierlo@wur.nl.

² The abbreviations used are: MG, molten globule; RNC, ribosome-nascent chain; ThT, thioflavin T; TEV, tobacco etch virus.

Molten Globule Formation on the Ribosome

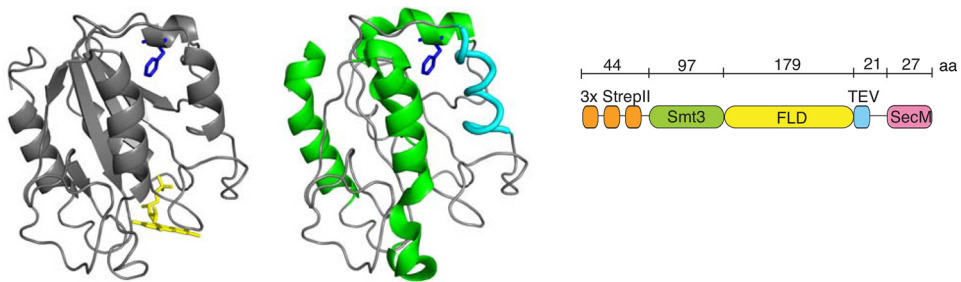


FIGURE 1. Differences between flavodoxin's native and MG structure and the construct used for RNC production. *Left*, schematic drawing of native flavodoxin (Protein Data Bank entry 1YOB (29)) with FMN colored yellow. Residue Phe-44 (blue) is shown in stick representation. *Middle*, schematic drawing of the four transiently structured regions of the off-pathway MG, which include α -helices (colored green) and structure that is neither α -helix nor β -strand (colored cyan) (33). These regions dock non-natively and form the core of apoflavodoxin's MG (33, 35, 39, 40). The schematic is a representation of structural elements in the MG and not of their packing. *Right*, construct for RNC production contains a triple N-terminal StrepII tag (orange), an Smt3 domain (green) fused to flavodoxin (yellow), a recognition site for TEV protease (blue), and a linker that spans the ribosomal exit tunnel and concludes with the SecM stalling sequence (magenta).

Under steady-state conditions, the MG is in equilibrium with native apoflavodoxin. Before formation of native apoflavodoxin can occur, the MG has to (partially) unfold. This unfolding is the rate-limiting step in folding of native apoflavodoxin. The cofactor FMN only binds to the flavin-binding site of natively folded apoflavodoxin (41). This binding can be followed in time by fluorescence spectroscopy, as FMN's fluorescence becomes severely quenched upon binding to native apoflavodoxin (42, 43).

Upon mixing FMN with apoflavodoxin under conditions where MG is present, cofactor binding and accompanied fluorescence quenching should be delayed, as the MG needs to unfold before native apoflavodoxin can form. This delayed FMN quenching is used in this study to reveal whether the ribosome modulates formation of molten globular apoflavodoxin. Previously, we demonstrated that once apoflavodoxin has been entirely synthesized and is exposed outside the ribosome, the protein is natively folded and capable of binding FMN (44). To demonstrate whether MGs form during translation, we take advantage of the following folding characteristic of flavodoxin variant F44Y (39); the apo-form of this variant switches from natively folded to the off-pathway MG upon decreasing ionic strength to physiological values (39, 40). Because of the higher thermodynamic stability of the holo-form of this protein, once apoflavodoxin binds FMN this topological switching no longer occurs (45). We prepared stalled RNC complexes that expose the entire F44Y flavodoxin protein outside the ribosomal exit tunnel. The translational stalling of the ribosomes is caused by an *Escherichia coli* SecM-derived peptide (46, 47), which we attached at the C terminus of flavodoxin. After purification of F44Y apoflavodoxin RNCs, we determined the corresponding FMN binding rates and thus the influence of the ribosome on MG formation.

Results

Dependence of Apoflavodoxin's Off-pathway MG on Ionic Strength and Temperature—Decreasing salt concentration is a well known method to destabilize folded proteins (48). Using this approach in F44Y apoflavodoxin samples, we can shift the equilibrium between natively folded protein and MG to the latter species (39). Fluorescence anisotropy shows that lowering ionic strength from 100 to 10 mM potassium PP_i (*i.e.* 345 to

75 mM equivalent NaCl units) at 25 °C forces F44Y apoprotein from native apoflavodoxin to the MG (Fig. 2A). The MG state is characterized by fluorescence anisotropy that is higher than native apoflavodoxin. In contrast, at high salt concentrations, as for example 100 mM potassium PP_i, F44Y apoflavodoxin is predominantly in its native state. For C69A apoflavodoxin, which is similar to wild-type apoflavodoxin (49, 50), no salt-dependent switch between folding states is observed (Fig. 2A), as its native state is considerably more stable than native F44Y apoflavodoxin (39).

The formation of the off-pathway MG not only depends on ionic strength but also on temperature. To follow the temperature-dependent existence of this MG, we added the extrinsic dye ThT. This reporter molecule is commonly employed to follow amyloid fibril formation, as it has a high affinity for β -sheets. Upon binding to fibrillar structures, ThT shows a fluorescence increase at 480 nm upon excitation at 450 nm. Binding of ThT and the subsequent fluorescence increase is not only restricted to fibrillar structures but can also occur due to the presence of non- β -sheet cavities, such as may form in MGs (25). Another extrinsic dye commonly used to probe MGs is 1-anilino-8-naphthalene sulfonate; however, in the case of F44Y apoflavodoxin, its fluorescence does not follow the unfolding of the MG, whereas ThT fluorescence does (data not shown).

Fig. 2B shows how temperature affects F44Y apoflavodoxin at high and low ionic strengths (*i.e.* 345 and 75 mM equivalent NaCl units, respectively). Temperature was raised from 15 to 45 °C, upon which F44Y apoflavodoxin unfolds (39). Temperature was not raised further to avoid formation of aggregates, which would lead to a rise in ThT fluorescence. For protein at low ionic strength and low temperature, ThT fluorescence is high (Fig. 2B), because F44Y apoflavodoxin is predominantly in the MG state. Upon increasing temperature, ThT fluorescence decreases non-cooperatively, because the MG unfolds gradually and binding of ThT diminishes. This gradual, non-cooperative unfolding is a typical feature of apoflavodoxin's MG (35, 37). Tryptophan fluorescence shows that the thermal unfolding transition of native F44Y apoflavodoxin in 100 mM potassium PP_i ranges from about 20 to 40 °C, with a thermal midpoint of 32.9 ± 0.3 °C (39). Above ~40 °C, ThT fluorescence of protein

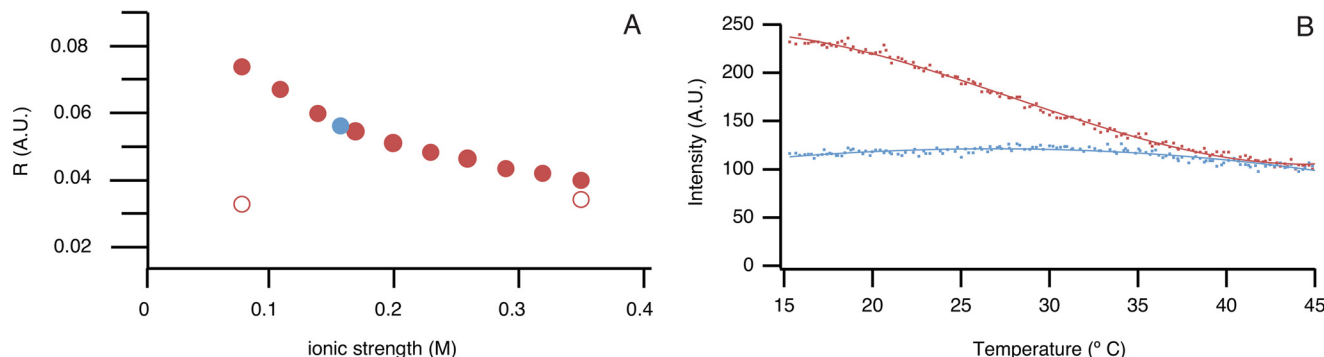


FIGURE 2. Effects of ionic strength or temperature on F44Y apoflavodoxin. *A*, ionic strength dependence of fluorescence anisotropy of F44Y (closed red circles) and C69A apoflavodoxin (open red circles) (graph adapted from Ref. 39). Upon decreasing ionic strength F44Y apoflavodoxin forms a MG, which is characterized by fluorescence anisotropy that is higher than native apoflavodoxin. Expected anisotropy of F44Y apoflavodoxin in buffer I is shown as a blue circle. *B*, temperature dependence of ThT binding to F44Y apoflavodoxin, as followed by fluorescence emission at 485 nm. Protein is in 10 (red) or 100 mM (blue) potassium PP_i, pH 6.0. ThT binding to the MG of F44Y apoflavodoxin increases ThT fluorescence. Because of unfolding of the MG with increasing temperature, ThT releases, and its fluorescence decreases. Protein concentration is 3.3 μ M, and the heating rate is 1 $^{\circ}$ C/min.

at low and high salt concentrations is similar, because at both conditions the protein is now unfolded. At a high salt concentration, a slight hump in ThT fluorescence is observed in the thermal unfolding transition of native protein (Fig. 2*B*). This hump arises because the MG state of F44Y apoflavodoxin populates. At the thermal midpoint of native apoflavodoxin (*i.e.* 32.9 ± 0.3 $^{\circ}$ C), ThT fluorescence due to MG population is low because the MG is gradually unfolded.

Fig. 2*B* implies that at a low salt concentration, the MG of F44Y apoflavodoxin is maximally populated at about 15 $^{\circ}$ C. This corroborates our previous findings that the off-pathway MG of F44Y apoflavodoxin is structured in the absence of denaturant (35, 40).

FMN Binding Rate as a Tool to Reveal the Presence of Apoflavodoxin's MG—FMN is essential for flavodoxin's role in electron transport. This cofactor binds to native apoflavodoxin through a very specific combination and geometry of aromatic and hydrogen bond interactions (41, 45). In native apoflavodoxin, the flavin-binding site is flexible, whereas upon cofactor incorporation it becomes rather rigid (45, 51, 52). Cofactor binding not only influences the binding pocket itself but also affects residues far away, resulting in picomolar binding affinity of FMN (45). As a consequence, flavodoxin is thermodynamically very stable and has to first release FMN before it can unfold (41, 45). Accordingly, FMN binding to native apoflavodoxin is the last step during folding of flavodoxin. FMN neither acts as a nucleation site for folding nor does it interact with folding intermediates of apoflavodoxin, including the discussed off-pathway MG (41).

Binding of FMN to native apoflavodoxin can be followed by FMN fluorescence, as FMN incorporation into native apoflavodoxin severely quenches its fluorescence. We demonstrate this phenomenon in Fig. 3*A*, which shows the time-dependent decrease of FMN fluorescence upon cofactor binding to C69A apoflavodoxin in 100 and 10 mM potassium PP_i at 25 $^{\circ}$ C. The rates of FMN binding at both salt concentrations are identical, because C69A apoflavodoxin is natively folded under these circumstances (39).

In contrast to C69A apoflavodoxin, the rates of FMN binding to F44Y apoflavodoxin in 100 and 10 mM potassium PP_i differ drastically (Fig. 3*B*). This dissimilarity arises because F44Y apo-

flavodoxin in 100 mM potassium PP_i is natively folded, whereas in 10 mM potassium PP_i the protein extensively populates the off-pathway MG. As this MG needs to unfold before productive folding can take place, FMN binding is delayed significantly when compared with F44Y apoflavodoxin in 100 mM potassium PP_i and C69A apoflavodoxin in 10 or 100 mM potassium PP_i, respectively. Thus, ascertaining the rate of FMN binding to apoflavodoxin as a function of ionic strength is a suitable tool to detect the presence of apoflavodoxin's off-pathway MG.

To preserve ribosomal integrity during purification of RNCs, we use buffer I (50 mM HEPES-KOH, 100 mM potassium acetate, 15 mM magnesium acetate, 1 mM dithiothreitol (DTT), pH 7.4), which contains magnesium to hold the two ribosomal subunits together. At the ionic strength of buffer I, which is similar to that of the cellular environment, the MG state of F44Y apoflavodoxin populates (Fig. 2*A*). We therefore assessed the rate of FMN binding to F44Y apoflavodoxin in buffer I (Fig. 3*C*). When compared with F44Y apoflavodoxin in 100 mM potassium PP_i, the FMN binding rate is considerably reduced in buffer I, indicating the presence of significant amounts of MG. To confirm that ionic strength also affects the equilibrium between MG and native apoflavodoxin in buffer I, 290 mM NaCl was added to buffer I, which would approximate the ionic strength of 100 mM potassium PP_i. Indeed, the FMN binding rate increases upon addition of salt to buffer I and becomes comparable with the rate found for native apoflavodoxin.

Production and Purification of RNCs of F44Y Flavodoxin in Vivo—To assess whether MGs form during translation, we produced RNCs of C69A and F44Y flavodoxin in *E. coli* (called C69A_{RNC} and F44Y_{RNC}, respectively), using the construct of Fig. 1, *right*. Production at 37 $^{\circ}$ C and purification of C69A_{RNC} have been described elsewhere (44). In case of F44Y_{RNC} we use the same procedure, except that now RNCs are induced in *E. coli* at either 37 or 15 $^{\circ}$ C. Lowering the temperature to 15 $^{\circ}$ C maximizes population of the MG state of F44Y apoflavodoxin, whereas at 37 $^{\circ}$ C the protein is unfolded (Fig. 2*B*).

Although the SecM sequence allows for relatively tight stalling (46), some release of nascent chains happens during their production in *E. coli*, as we observed previously for RNCs of C69A flavodoxin (44). This release is most probably due to the physical force that is exerted as soon as the nascent chain folds

Molten Globule Formation on the Ribosome

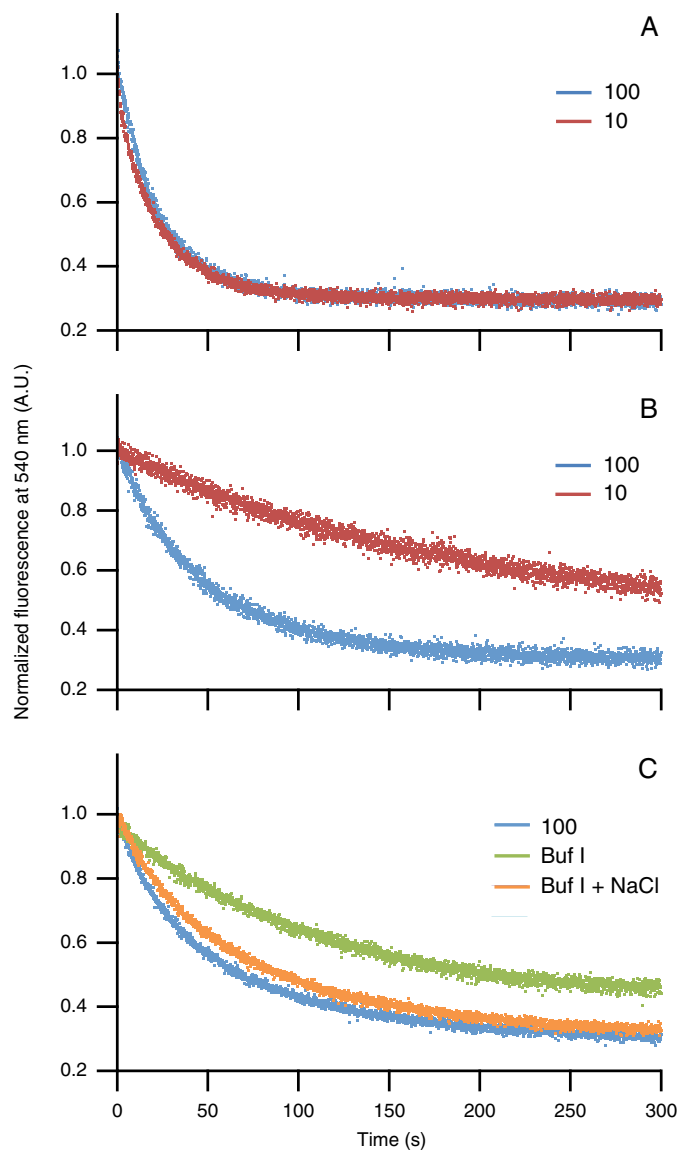


FIGURE 3. Rate with which FMN binds to apo-ribosomally nascent C69A and F44Y flavodoxin depends on the presence of molten globular protein and thus on the salt concentration.

To follow quenching of flavin fluorescence, FMN is added to protein at 25 °C. Shown are normalized FMN fluorescence traces. A, C69A apo-ribosomally nascent C69A protein is natively folded under both conditions and thus binds FMN with the same rate. Concentrations for protein and FMN are 140 and 25 nM, respectively. B, F44Y apo-ribosomally nascent F44Y protein is natively folded, whereas in 10 mM potassium PP_i, the F44Y variant predominantly populates the MG state, which delays FMN binding as the MG needs to unfold before native apo-ribosomally nascent C69A protein can form. Concentrations for F44Y apo-ribosomally nascent F44Y protein and FMN are 71 and 25 nM, respectively. C, F44Y apo-ribosomally nascent F44Y protein in 100 mM potassium PP_i (blue) and in buffer I (green) containing 290 mM NaCl (orange). Protein is natively folded under these conditions and thus binds FMN with similar rate. F44Y apo-ribosomally nascent F44Y protein in buffer I (green) populates the MG state, thereby delaying FMN binding. Concentrations of F44Y apo-ribosomally nascent F44Y protein and FMN are 62 and 25 nM, respectively.

(53, 54). Binding of FMN to natively folded nascent chains does not dissociate nascent flavodoxin from the ribosome (44). To separate released protein (called C69A_P or F44Y_P) from RNCs (*i.e.* C69A_{RNC} or F44Y_{RNC}), we utilize size-exclusion chromatography. The absorbance ratio $A_{260}:A_{280}$ enables distinction between RNCs and released flavodoxin, as this ratio is ~ 2 for RNCs, although $A_{260}:A_{280}$ is <1 for released protein. The RNCs

elute in the void volume of the Superdex75 column, whereas released protein elutes later. Fig. 4A illustrates this separation of C69A_{RNC} and C69A_P through size exclusion. A similar distribution is observed for the F44Y flavodoxin variant grown at 37 °C (Fig. 4B), showing that also in case of this protein variant release of nascent chains happens. However, an additional third elution peak is now present. This extra peak arises from the protein fragment consisting of the triple StrepII tag and Smt3 domain (Fig. 4, B and C), which we refer to as the Smt3 fragment. The identity of the 18-kDa fragment is confirmed by Western blotting probed with antibodies against the StrepII tag (Fig. 4D). Because the remaining C-terminal fragments no longer contain a StrepII tag, they are not present after the purification step using a Strep-Tactin column. We previously observed the same degradation product for C-terminally shortened nascent chains of C69A flavodoxin. These shortened proteins are less stable relative to the full-length C69A protein (44), and thus Fig. 4, B and C, also indicates decreased stability of both F44Y_{RNC} and/or F44Y_P when produced at 15 or 37 °C. Whether intracellular degradation of the F44Y construct occurs while it is bound to the ribosome and/or while it has been released is unknown. We can only distinguish between both species after their separation using size-exclusion chromatography. Since degradation had already happened, we were unable to determine which species degraded and formed the observed Smt3 fragment.

Production of the F44Y flavodoxin construct at 15 °C does not alter the elution peak arising from the Smt3 fragment (Fig. 4C). Thus, a temperature change of 37 to 15 °C has no effect on the amount of *in vivo* proteolytic degradation of F44Y_{RNC} and/or F44Y_P, suggesting that the respective proteolytic susceptibility of nascent chain and released protein is similar at both temperatures. The ratio between F44Y_P and F44Y_{RNC} is calculated taking into account the differences in extinction coefficients at 280 nm of RNCs and released protein. At both temperatures the ratio is around 70, which is comparable with the ratio we have found previously for a C-terminally shortened nascent chain of C69A flavodoxin (44).

All Purified F44Y_P Contains FMN—In a previous study, we showed that when FMN binds to a released C-terminally shortened C69A flavodoxin construct, this construct is protected against intracellular proteolysis, due to the increased thermodynamic stability conferred by incorporated FMN (44). As a consequence, all of these released constructs were saturated with FMN, because the unstable apo-forms are proteolytically degraded in *E. coli* (causing the appearance of the Smt3 fragment). In contrast, for C69A_P, which is full-length protein construct, the FMN content varies between 40 and 100%, depending on the *E. coli* batch used for purification (44). Because of its increased thermodynamic stability compared with C-terminally shortened constructs, the apo-form of C69A_P is not proteolytically degraded. To verify in this study whether the elution peak labeled F44Y_P arises from protein saturated with cofactor, we titrated this fraction with FMN (Fig. 5A). Because of quenching of FMN fluorescence upon cofactor binding to apo-protein, the slope of fluorescence data arising from FMN bound to protein is less steep than the slope resulting from free FMN. This characteristic is widely used to demonstrate FMN binding

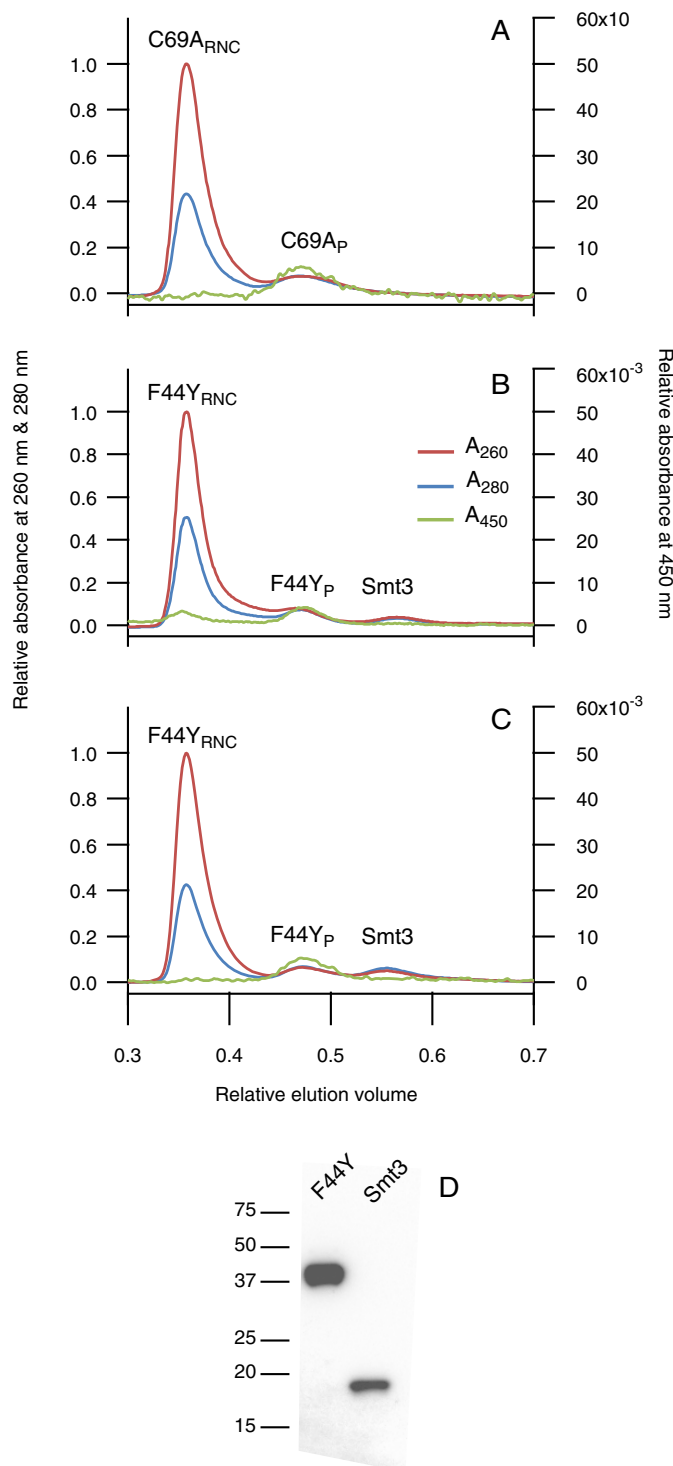


FIGURE 4. Comparison of release and degradation of C69A and F44Y flavodoxin nascent chains produced in *E. coli* under several growth conditions. Shown are Superdex75 elution profiles, with absorbance at 260 (red), 280 (blue), and 450 nm (green). All absorbance traces are normalized relative to the maximum absorbance at 260 nm of the respective RNCs. Absorbance at 450 nm tracks FMN incorporation. Elution volumes are normalized to the total column volume V_t . All constructs are induced for 2.5 h in *E. coli* *Δtig:kan* in minimal medium at either 37 °C (A and B) or 15 °C (C). A, use of C69A flavodoxin construct produces C69A_{RNC} and C69A_P. B, use of F44Y flavodoxin construct produces F44Y_{RNC} and F44Y_P. Proteolytic degradation of F44Y protein construct results in the presence of the fragment triple StrepII tag-Smt3 (labeled Smt3). C, use of F44Y flavodoxin construct at 15 °C produces F44Y_{RNC} and F44Y_P with the same degradation pattern (i.e. Smt3) as observed in (B). D, Western blot of the fractions labeled F44Y and Smt3 probed with antibodies against the N-terminal StrepII tag.

(42, 43, 45). Fig. 5A reveals similar slopes for FMN fluorescence titration data of buffer and F44Y_P. This observation shows that F44Y_P binds no additional FMN.

To determine the ratio of FMN to apoprotein, we added trichloroacetic acid (TCA) to F44Y_P. This dissociates the cofactor from the protein, and after centrifugation, we measured FMN fluorescence of the supernatant. This experiment demonstrates equimolar presence of FMN and apoprotein (Fig. 5B). Full saturation of F44Y_P with FMN was seen independent of production temperature (i.e. 15 or 37 °C). Finally, we followed FMN fluorescence in time upon addition of the cofactor to F44Y_P (Fig. 5C). If the sample would contain any F44Y_P in its apo-form, one should detect a decrease in FMN fluorescence upon FMN binding. However, no such decrease was observed and thus no cofactor binding happened.

In conclusion, binding of FMN protects destabilized apoflavodoxin variants against the action of intracellular proteases, and thus all F44Y_P we purify contains FMN.

F44Y_{RNC} Isolated from *E. coli* Is Saturated with FMN—To determine the extent of cofactor incorporation into F44Y_{RNC}, we performed a titration of the purified nascent protein with FMN. Fig. 5A shows that no added FMN binds to these RNCs. TCA precipitation of RNCs shows that this observation arises because RNCs of F44Y flavodoxin contain FMN (Fig. 5B), regardless of whether they are produced by *E. coli* at 15 or 37 °C. We observe only a marginal decrease in FMN fluorescence after addition of the cofactor to F44Y_{RNC} (Fig. 5C). This decrease corresponds to maximally 5% of F44Y_{RNC} being in the apo-form. In contrast to the observed nearly full saturation of F44Y_{RNC} with FMN, we previously demonstrated that C69A_{RNC} is purified from *E. coli* as apoprotein. Observation of an altering slope in FMN fluorescence titration data shows that C69A_{RNC} binds FMN (Fig. 5A). This difference in FMN occupation of F44Y_{RNC} and C69A_{RNC}, and the observation that F44Y_P is fully saturated with FMN, suggests that when the apo-form of F44Y protein is present in *E. coli*, it is not as stable in the cellular environment of *E. coli* as C69A apoprotein is. Therefore, only the holo-forms of RNCs and released F44Y protein are purified.

Domains of F44Y_P Do Not Affect MG Formation of Apoflavodoxin—To assess whether the triple Strep tag, the Smt3 domain, the linker, and the SecM sequence (Fig. 1, right) influence MG formation of F44Y apoflavodoxin, we removed FMN from purified F44Y_P according to a previously published procedure (44). Subsequently, the FMN binding trace of this refolded apo-F44Y_P was measured in various buffers (Fig. 5D). Comparison of the refolded apo-F44Y_P traces with those of F44Y apoflavodoxin (Fig. 3C) shows that for both proteins a change in ionic strength has a similar effect on FMN binding. Increasing potassium PP_i concentration from 10 to 100 mM, or addition of 290 mM NaCl to buffer I, leads to an increase in FMN binding rate. This observation is due to increased population of the native state of apoflavodoxin. Upon addition of salt (buffer I with 290 mM NaCl), the FMN binding rate of apo-F44Y_P is similar to the rate observed for apo-F44Y_P in 100 mM potassium PP_i, as both proteins are natively folded. Thus, the presence of the triple Strep tag, the Smt3 domain, the linker, and the SecM sequence of the construct used for RNC produc-

Molten Globule Formation on the Ribosome

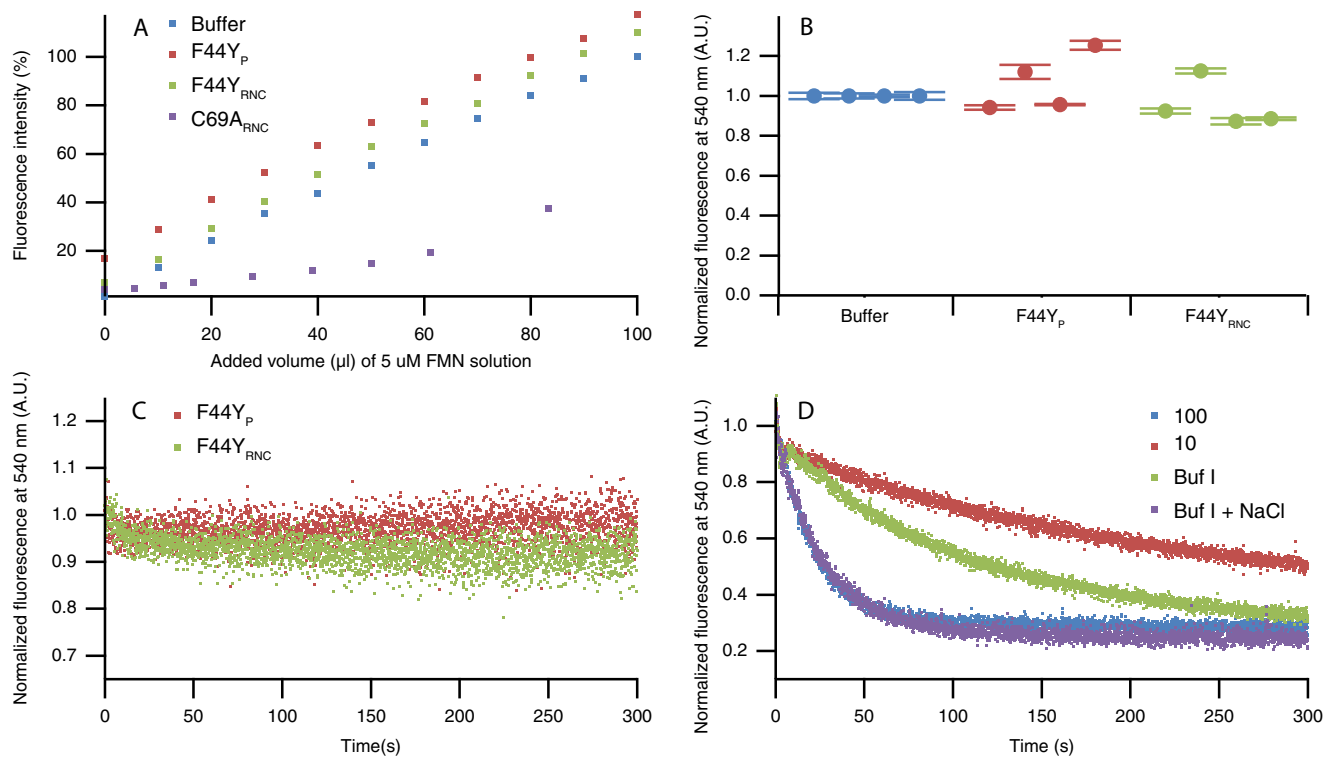


FIGURE 5. RNCs of F44Y flavodoxin construct and released protein construct isolated from *E. coli* are saturated with FMN. *A*, titration of buffer I, F44Y_P, F44Y_{RNC}, and C69A_{RNC} with FMN. Observation of an altering slope in FMN fluorescence titration data reveals cofactor binding, as is the case for C69A_{RNC}. F44Y_P and F44Y_{RNC} show no change in slope of FMN fluorescence titration data. All fluorescence is normalized to the fluorescence of the end point of the titrated buffer sample. Concentration of protein and RNC is 0.5 μM. Data of C69A_{RNC} are adapted from Ref. 44. *B*, fluorescence of FMN in supernatants of F44Y_P (red) and F44Y_{RNC} (green) after TCA precipitation. The average fluorescence of TCA samples of four purifications is shown, together with the corresponding standard deviation. Before addition of TCA, concentration of F44Y_P and F44Y_{RNC} was 50 nM. Fluorescence is normalized to fluorescence of buffer I containing 50 nM FMN (blue). *C*, FMN binding traces of F44Y_P and F44Y_{RNC} isolated from *E. coli*. FMN fluorescence is normalized. F44Y_P, F44Y_{RNC}, and FMN concentrations are 50, 50, and 25 nM, respectively. *D*, triple Strep tag, Smt3 domain, the linker, and the SecM sequence of the construct used for RNC production do not influence the formation of the off-pathway MG of apoflavodoxin. Shown are FMN binding traces of apo-F44Y_P in 100 mM potassium PP₂ (blue), 10 mM potassium PP₂ (red), buffer I (green), and buffer I (Buf I) + 290 mM NaCl (purple). F44Y_P and FMN concentrations are 147 and 25 nM, respectively.

tion does not influence formation of the off-pathway MG of apoflavodoxin or impair FMN binding.

Ribosome Forces Entirely Synthesized and Fully Exposed F44Y Apoflavodoxin toward the Native State—Because no apo-F44Y_{RNC} could be obtained from *E. coli* due to proteolytic degradation, we adopted an *in vitro* transcription/translation approach to generate nascent F44Y constructs in their apo-form. We used a highly pure *in vitro* protein synthesis kit (PUR-Express[®] Δ (aa, tRNA), New England Biolabs) to preclude the presence of FMN in the translation reaction. We avoided usage of *E. coli* extracts for *in vitro* protein synthesis, as FMN is difficult to remove from these extracts. The highly purified *in vitro* protein synthesis kit does not contain chaperones that interact with nascent chains, such as trigger factor and DnaK.

In vitro protein synthesis yields a very low percentage of stalled ribosomes, as can be inferred from Fig. 6A. Shown is a Coomassie-stained gel of a sample from an *in vitro* translation reaction before and after purification with Strep-Tactin column chromatography. The gel of the sample before purification shows protein bands originating from ribosomal proteins. Also, bands arising from non-ribosomal components of the *in vitro* translation kit, like aminoacyl-tRNA synthases, can be seen. These non-ribosomal components can be removed by Strep-Tactin column chromatography. In Fig. 6A the position of the band corresponding to F44Y protein construct is indicated. The

identity of this band is verified by Western blottings probed with antibodies against flavodoxin and StrepII tag (Fig. 6B). Before purification of the *in vitro* translation mixture, this band was barely visible, as most ribosomes were devoid of stalled nascent chains. After Strep-Tactin chromatography purification, the intensity of this band was comparable with those of ribosomal proteins, because in stalled RNCs all proteins are present in equimolar quantities.

In contrast, F44Y flavodoxin nascent chains produced in *E. coli* are released from the ribosome in considerable quantities, as described above (Fig. 4, *B* and *C*). Interestingly, the amount of F44Y_P produced *in vitro* is very small, because, as mentioned, Fig. 6A shows that the Coomassie-stained bands of F44Y flavodoxin RNCs are all of comparable intensities. In case of nascent chain release, the released construct would have been purified together with the remaining RNCs by Strep-Tactin chromatography. Essentially, F44Y flavodoxin construct would be overproduced and would therefore no longer be equimolar to ribosomal proteins, which is clearly not the case (Fig. 6A).

As discussed, determination of the FMN binding rate enables detection of the presence of apoflavodoxin's MG. This methodology is thus suitable to investigate formation of molten globular nascent apoflavodoxin, provided that ribosomes themselves do not bind FMN. To check the latter, FMN was added to puri-

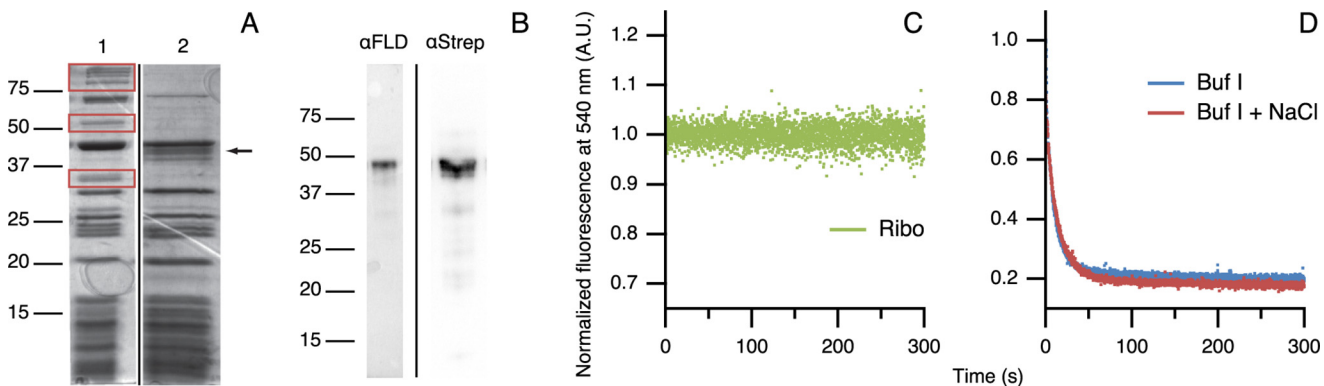


FIGURE 6. Apoflavodoxin in F44Y_{RNC} is natively folded at low and high salt concentrations. *A*, Coomassie-stained gels of samples taken from an *in vitro* translation reaction of F44Y flavodoxin construct before (Lane 1) and after (Lane 2) purification with Strep-Tactin affinity chromatography. An arrow labels the position of F44Y flavodoxin construct, and red boxes enclose the bands of the non-ribosomal components of the *in vitro* translation reaction. *B*, Western blotting of sample (2), probed with antibodies against flavodoxin (α FLD) or N-terminal StrepII tag (α Strep), respectively. *C*, FMN fluorescence shows that ribosomes (Ribo) do not bind FMN. Concentrations of ribosomes and FMN are 50 and 25 nm, respectively. A.U., arbitrary units. *D*, FMN binding traces of F44Y_{RNC} in buffer I (blue) and in this buffer with 290 mM NaCl (red). Concentrations of F44Y_{RNC} and FMN are 50 and 25 nm, respectively.

fied *E. coli* ribosomes, and its fluorescence followed in time. As can be inferred from Fig. 6C, FMN does not associate with ribosomes, because no change in flavin fluorescence is observed.

We assessed the rate of FMN binding to F44Y_{RNC} in buffer I and in this buffer with 290 mM NaCl. Fig. 6D shows that this increase in salt concentration does not affect the rate of FMN binding to F44Y_{RNC}. In contrast, such salt concentration change of buffer I considerably increases the rate of FMN binding to F44Y apoflavodoxin (Fig. 3C) and to the apo-form of F44Y_P (Fig. 5D), as F44Y apoflavodoxin switches from MG to native protein. Because F44Y_{RNC} binds FMN rapidly at both salt concentrations, apoflavodoxin in F44Y_{RNC} must be natively folded under both conditions. We note that another implication of this observation is that the sample of F44Y_{RNC} cannot contain the released F44Y flavodoxin construct, because if this would be the case the mentioned increase in salt concentration would lead to a change in FMN binding rate. Such a change is not seen in Fig. 6D, thereby corroborating the above-mentioned equimolar presence of nascent chain and ribosomal proteins. At low ionic strength, F44Y apoflavodoxin and the apo-form of F44Y_P are molten globular, but, remarkably, apoflavodoxin in F44Y_{RNC} is natively folded. Apparently, the ribosome modulates flavodoxin folding and forces F44Y apoflavodoxin that is entirely synthesized and exposed outside the ribosome, to which it is stalled by an artificial linker containing the SecM sequence, toward the native state. To our knowledge, this is the first time the effect of the ribosome on formation of MGs during protein synthesis has been determined.

Discussion

Determination of the rate of flavin binding is an innovative approach that makes it possible to investigate the presence of MGs during translation of flavin-binding proteins. Using this methodology, we demonstrated that the ribosome forces nascent and fully exposed F44Y apoflavodoxin toward the native state. Confinement of MG formation during translation is an important observation that emphasizes differences between folding *in vivo* and *in vitro*.

Because of the presence of ribosomal RNA surrounding the end of the exit tunnel, this part of the ribosome area has a

considerable negative surface charge (55). Although some proteins only seem to randomly interact with the ribosomal surface (56), others interact to such an extent that local motions of compact domains are constrained (57) or folding/unfolding transitions are slowed down (58). These interactions likely arise due to attraction of positively charged residues and simultaneous repulsion of negatively charged residues of the nascent chain by the negatively charged ribosomal outer surface. Because the population of natively folded apoflavodoxin within F44Y_{RNC} at a low salt concentration (*i.e.* in buffer I) is higher than is the case for F44Y apoflavodoxin in buffer I, the ribosome restrains formation of the off-pathway MG. Upon release of the nascent chain this effect is negated, as F44Y_P, a construct that was stalled to the ribosome before its release due to physical exertion, can form the MG state upon lowering ionic strength (Fig. 5D). It is tempting to speculate that the ribosome potentially mimics the effects of high ionic strength, thereby forcing molten globular apoflavodoxin to the native state. Native apoflavodoxin has a net charge of -13 at neutral pH (59). Possibly, the conformational space of unfolded nascent apoflavodoxin is restricted due to electrostatic repulsion of the nascent chain by the ribosomal surface, leading to entropic stabilization of native protein at physiological ionic strength.

We note that the RNC construct we use creates a somewhat artificial situation compared with translation of solely the flavodoxin gene. Because of the presence of the SecM sequence and attached linker (Fig. 1, *right*), RNCs are produced with the entire flavodoxin domain exposed outside the ribosome. In contrast, when a ribosome reaches the stop codon and terminates the nascent chain during translation of solely the flavodoxin domain, $\sim 30-40$ residues of the protein are still buried in the exit tunnel. These residues need to traverse this tunnel before full-length protein emerges from the ribosome. We showed based on investigating C-terminally shortened flavodoxin RNCs that exposure of the five C-terminal residues of flavodoxin is essential for the nascent chain to be able to attain its native fold (44). Thus, although the 30–40 C-terminal residues of flavodoxin are inside the exit tunnel, the part of the

protein that is already outside the exit tunnel is unable to fold natively.

It would be interesting to verify whether our finding that the ribosome forces flavodoxin toward the native state also applies to the folding of flavodoxin-like domains within multidomain proteins like cytochrome P450 reductase and nitric-oxide synthase (60, 61). As each domain of such a protein is translated the nascent chain remains tethered to the ribosome, thus providing the ribosome ample opportunity to influence the folding of an already translated flavodoxin-like domain.

Experimental Procedures

Protein Expression and Purification—To avoid covalent dimerization of purified *A. vinelandii* (apo)flavodoxin, the single cysteine at position 69 was substituted by an alanine (50). The C69A variant is similar to wild-type (apo)flavodoxin (49, 50). An additional F44Y mutation was introduced (39), and this protein variant is referred to as F44Y (apo)flavodoxin. Both constructs were transformed in *E. coli* (strain TG2) and purified as described previously (50). Apoprotein was prepared according to established protocols (44). Apoprotein concentrations were determined by titration with known amounts of FMN. Purified proteins in 100 mM potassium pyrophosphate (potassium PP_i) buffer, pH 6.0, were flash-frozen in liquid nitrogen and stored at -80 °C.

Because of cold denaturation, some F44Y apoflavodoxin deteriorates into soluble molecules that are incapable of binding FMN upon thawing. These molecules cannot be separated from FMN binding-competent apoflavodoxin, and thus the latter concentration was determined by titration with FMN in 100 mM potassium PP_i, pH 6.0. Also, as much as possible, freshly prepared F44Y apoflavodoxin was used in experiments.

Influence of Temperature on Full-length Isolated Protein—Thermal unfolding of F44Y apoflavodoxin was probed by ThT fluorescence using a Cary Eclipse spectrophotometer (Varian). Excitation was at 445 nm, and emission was measured at 485 nm. Temperature was increased from 15 to 45 °C at a rate of 1 °C/min. The excitation and emission slits were set to bandwidths of 5 and 10 nm, respectively, and the PMT voltage was 900 V. 3.3 μM F44Y apoflavodoxin and 56 μM ThT (Sigma) were used in 10 or 100 mM potassium PP_i, pH 6.0.

Engineering RNC Variants—Plasmids for RNC production contain a sequence coding for a triple N-terminal StrepII tag, an Smt3 domain, a TEV site, a linker, and a SecM stalling motif (Fig. 1, right). The flavodoxin sequence (C69A or F44Y) was inserted in the multiple cloning site present between the Smt3 domain and the TEV site. Ulp1 protease specifically recognizes the Smt3 domain and cleaves downstream from this domain, thereby producing nascent flavodoxin chains with Ala-1 as the authentic N terminus, if required. The recognition site for TEV protease enables release of nascent protein from the ribosome. The plasmid was a kind gift of Professor Elke Deuerling (University of Konstanz, Germany) (56).

Expression and Purification of RNCs in Vivo and in Vitro—Plasmids were transformed in *E. coli* strain BL21(DE3) Δ*tig*:*kan* for expression of RNCs *in vivo*. All RNC variants were prepared as described previously (44). After growth of *E. coli* in Terrific Broth medium, cells were transferred to minimal (M9)

medium for expression of RNCs at either 37 or 15 °C for 1 h. RNCs were purified using Strep-Tactin-Sepharose (IBA GmbH) chromatography and subsequent size-exclusion (Superdex75) chromatography. RNCs and released protein chains were purified and stored in buffer I (50 mM HEPES-KOH, 100 mM potassium acetate, 15 mM magnesium acetate, 1 mM dithiothreitol (DTT), pH 7.4). After purification, the apo-form of released protein chains of F44Y flavodoxin was prepared in 100 mM potassium PP_i, pH 6.0, as described previously (44).

For *in vitro* expression of RNCs, the PURExpress® Δ (aa, tRNA) *in vitro* protein synthesis kit from New England Biolabs was used. The manufacturer's instructions were followed. After mixing the kit's components with the F44Y flavodoxin containing RNC plasmid, the reaction was allowed to proceed for 2 h at 37 °C. To purify RNCs produced *in vitro*, the reaction mixture was loaded onto a Strep-Tactin-Sepharose column and eluted as described previously in buffer I (44). Eluted RNCs were concentrated with a 10-kDa spin filter (EMD Millipore) at 5500 × g. Concentrated samples were frozen in liquid nitrogen and stored at -80 °C. Samples of each purification step were analyzed by Coomassie-stained SDS-PAGE or Western blotting using either flavodoxin antibody raised in rabbits (Eurogentec) followed by anti-rabbit HRP-IG (Eurogentec) or StrepMAB classic (IBA GmbH) against the N-terminal StrepII tag.

FMN Fluorescence—To establish FMN content of RNCs and released constructs, FMN titration or TCA precipitation was performed as described previously (44). To determine the MG nature of RNCs of F44Y protein and of released protein, binding of FMN to these molecules was followed in time. All flavin fluorescence experiments were measured on a Cary Eclipse spectrophotometer (Varian) at 25 °C.

Samples for FMN titration contained 0.5 μM of either RNC or released protein produced *in vivo* in buffer I. Samples were titrated with an FMN solution of 5 μM to determine their cofactor-binding capacity using flavin fluorescence. Excitation was at 450 nm, with emission recorded between 500 and 600 nm. For each titration point, the average of five scans was taken. Excitation and emission slits were set to a bandwidth of 5 nm, and PMT voltage was set to 900 V.

Samples for TCA precipitation contained 50 nM RNC or released protein produced *in vivo* in buffer I. To establish the total amount of FMN bound to protein, the samples were precipitated by adding 3% (w/v) TCA. Precipitate was spun down for 10 min at 21,000 × g at 4 °C, and the supernatant was carefully pipetted off to measure its flavin fluorescence. A 50 nM solution of FMN in 3% (w/v) TCA in buffer I was used as reference. Excitation was at 450 nm, with emission recorded between 500 and 600 nm. Each sample was scanned five times, and the average was used for calculations. Excitation and emission slits were set to a bandwidth of 10 or 20 nm, respectively. PMT voltage was set to 970 V.

To determine the rate of FMN binding to C69A and F44Y variants of apoflavodoxin, *E. coli* ribosomes (New England Biolabs), RNC, or released protein, samples were made of each with protein concentrations ranging from 50 to 147 nM. Samples were measured in stirred fluorescence cuvettes for 5 min before and after adding FMN to a final concentration of 24 nM. Excita-

tation was at 450 nm, and emission was monitored at 540 nm. Excitation and emission slits were set to bandwidths of 10 and 20 nm, respectively, and PMT voltage was 970 V. The averaging time of the measurement was 0.1 s. The time between addition of FMN and the start of fluorescence detection was \sim 2 s. Buffers used in these experiments were 10 mM potassium PP_i, pH 6.0, 100 mM potassium PP_i, pH 6.0, buffer I or buffer I with a final concentration of 290 mM NaCl. The latter buffer has an ionic strength equal to that of 100 mM potassium PP_i, pH 6.0.

Author Contributions—J. A. H., E. A., and A. H. W. expressed and purified flavodoxin variants and ribosomal nascent chain complexes. J. A. H. and A. H. W. acquired and analyzed the data. J. A. H., W. J. H. v. B., and C. P. M. v. M. wrote the manuscript.

References

1. Bryngelson, J. D., Onuchic, J. N., Soccia, N. D., and Wolynes, P. G. (1995) Funnels, pathways, and the energy landscape of protein folding: a synthesis. *Proteins* **21**, 167–195
2. Dill, K. A., and Chan, H. S. (1997) From Levinthal to pathways to funnels. *Nat. Struct. Biol.* **4**, 10–19
3. Jahn, T. R., and Radford, S. E. (2008) Folding versus aggregation: polypeptide conformations on competing pathways. *Arch. Biochem. Biophys.* **469**, 100–117
4. Dobson, C. M. (2003) Protein folding and misfolding. *Nature* **426**, 884–890
5. Ohgushi, M., and Wada, A. (1983) 'Molten-globule state': a compact form of globular proteins with mobile side-chains. *FEBS Lett.* **164**, 21–24
6. Kuroda, Y., Kidokoro, S., and Wada, A. (1992) Thermodynamic characterization of cytochrome *c* at low pH. Observation of the molten globule state and of the cold denaturation process. *J. Mol. Biol.* **223**, 1139–1153
7. Loh, S. N., Kay, M. S., and Baldwin, R. L. (1995) Structure and stability of a second molten globule intermediate in the apomyoglobin folding pathway. *Proc. Natl. Acad. Sci. U.S.A.* **92**, 5446–5450
8. Shastry, M. C., and Udgaonkar, J. B. (1995) The folding mechanism of barstar: evidence for multiple pathways and multiple intermediates. *J. Mol. Biol.* **247**, 1013–1027
9. Arai, M., and Kuwajima, K. (2000) Role of the molten globule state in protein folding. *Adv. Protein Chem.* **53**, 209–282
10. Ptitsyn, O. B., Pain, R. H., Semisotnov, G. V., Zerovnik, E., and Razgulyaev, O. I. (1990) Evidence for a molten globule state as a general intermediate in protein folding. *FEBS Lett.* **262**, 20–24
11. Bollen, Y. J., and van Mierlo, C. P. (2005) Protein topology affects the appearance of intermediates during the folding of proteins with a flavodoxin-like fold. *Biophys. Chem.* **114**, 181–189
12. Bhattacharyya, S., and Varadarajan, R. (2013) Packing in molten globules and native states. *Curr. Opin. Struct. Biol.* **23**, 11–21
13. Baldwin, R. L., and Rose, G. D. (2013) Molten globules, entropy-driven conformational change and protein folding. *Curr. Opin. Struct. Biol.* **23**, 4–10
14. van der Goot, F. G., González-Mañas, J. M., Lakey, J. H., and Pattus, F. (1991) A 'molten-globule' membrane-insertion intermediate of the pore-forming domain of colicin A. *Nature* **354**, 408–410
15. van der Goot, F. G., Lakey, J. H., and Pattus, F. (1992) The molten globule intermediate for protein insertion or translocation through membranes. *Trends Cell Biol.* **2**, 343–348
16. Lally, E. T., Hill, R. B., Kieba, I. R., and Korostoff, J. (1999) The interaction between RTX toxins and target cells. *Trends Microbiol.* **7**, 356–361
17. Ellis, J. P., Bakke, C. K., Kirchdoerfer, R. N., Jungbauer, L. M., and Cavagnero, S. (2008) Chain dynamics of nascent polypeptides emerging from the ribosome. *ACS Chem. Biol.* **3**, 555–566
18. Evans, M. S., Sander, I. M., and Clark, P. L. (2008) Cotranslational folding promotes β -helix formation and avoids aggregation *in vivo*. *J. Mol. Biol.* **383**, 683–692
19. Cabrita, L. D., Hsu, S.-T., Launay, H., Dobson, C. M., and Christodoulou, J. (2009) Probing ribosome-nascent chain complexes produced *in vivo* by NMR spectroscopy. *Proc. Natl. Acad. Sci. U.S.A.* **106**, 22239–22244
20. Hoffmann, A., Becker, A. H., Zachmann-Brand, B., Deuerling, E., Bokau, B., and Kramer, G. (2012) Concerted action of the ribosome and the associated chaperone trigger factor confines nascent polypeptide folding. *Mol. Cell* **48**, 63–74
21. Kelkar, D. A., Khushoo, A., Yang, Z., and Skach, W. R. (2012) Kinetic analysis of ribosome-bound fluorescent proteins reveals an early, stable, cotranslational folding intermediate. *J. Biol. Chem.* **287**, 2568–2578
22. Lamprou, P., Kempe, D., Katranidis, A., Büldt, G., and Fitter, J. (2014) Nanosecond dynamics of calmodulin and ribosome-bound nascent chains studied by time-resolved fluorescence anisotropy. *ChemBioChem* **15**, 977–985
23. Holtkamp, W., Kokic, G., Jäger, M., Mittelstaet, J., Komar, A. A., and Rodnina, M. V. (2015) Cotranslational protein folding on the ribosome monitored in real time. *Science* **350**, 1104–1107
24. Jaenicke, R., and Seckler, R. (1997) Protein misassembly *in vitro*. *Adv. Protein Chem.* **50**, 1–59
25. Hawe, A., Sutter, M., and Jiskoot, W. (2008) Extrinsic fluorescent dyes as tools for protein characterization. *Pharm. Res.* **25**, 1487–1499
26. Engelhard, M., and Evans, P. A. (1996) Experimental investigation of side-chain interactions in early folding intermediates. *Fold. Des.* **1**, R31–R37
27. Plaxco, K. W., and Dobson, C. M. (1996) Time-resolved biophysical methods in the study of protein folding. *Curr. Opin. Struct. Biol.* **6**, 630–636
28. Chakraborty, S., Ittah, V., Bai, P., Luo, L., Haas, E., and Peng, Z. (2001) Structure and dynamics of the α -lactalbumin molten globule: fluorescence studies using proteins containing a single tryptophan residue. *Biochemistry* **40**, 7228–7238
29. Alagaratnam, S., van Pouderoyen, G., Pijning, T., Dijkstra, B. W., Cavazzini, D., Rossi, G. L., Van Dongen, W. M., van Mierlo, C. P., van Berkel, W. J., and Canters, G. W. (2005) A crystallographic study of Cys69Ala flavodoxin II from *Azotobacter vinelandii*: structural determinants of redox potential. *Protein Sci.* **14**, 2284–2295
30. Caetano-Anollés, G., Kim, H. S., and Mittenthal, J. E. (2007) The origin of modern metabolic networks inferred from phylogenomic analysis of protein architecture. *Proc. Natl. Acad. Sci. U.S.A.* **104**, 9358–9363
31. Bollen, Y. J., Sánchez, I. E., and van Mierlo, C. P. (2004) Formation of on- and off-pathway intermediates in the folding kinetics of *Azotobacter vinelandii* apoflavodoxin. *Biochemistry* **43**, 10475–10489
32. Bollen, Y. J., Kamphuis, M. B., and van Mierlo, C. P. (2006) The folding energy landscape of apoflavodoxin is rugged: hydrogen exchange reveals nonproductive misfolded intermediates. *Proc. Natl. Acad. Sci. U.S.A.* **103**, 4095–4100
33. Nabuurs, S. M., Westphal, A. H., and van Mierlo, C. P. (2008) Extensive formation of off-pathway species during folding of an α - β parallel protein is due to docking of (non)native structure elements in unfolded molecules. *J. Am. Chem. Soc.* **130**, 16914–16920
34. Visser, N. V., Westphal, A. H., van Hoek, A., van Mierlo, C. P., Visser, A. J., and van Amerongen, H. (2008) Tryptophan-tryptophan energy migration as a tool to follow apoflavodoxin folding. *Biophys. J.* **95**, 2462–2469
35. Nabuurs, S. M., Westphal, A. H., and van Mierlo, C. P. (2009) Noncooperative formation of the off-pathway molten globule during folding of the α - β parallel protein apoflavodoxin. *J. Am. Chem. Soc.* **131**, 2739–2746
36. Lindhoud, S., Westphal, A. H., Visser, A. J., Borst, J. W., and van Mierlo, C. P. (2012) Fluorescence of Alexa fluor dye tracks protein folding. *PLoS One* **7**, e46838
37. Lindhoud, S., Pirchi, M., Westphal, A. H., Haran, G., and van Mierlo, C. P. (2015) Gradual folding of an off-pathway molten globule detected at the single-molecule level. *J. Mol. Biol.* **427**, 3148–3157
38. Engel, R., Westphal, A. H., Huberts, D. H., Nabuurs, S. M., Lindhoud, S., Visser, A. J., and van Mierlo, C. P. (2008) Macromolecular crowding compacts unfolded apoflavodoxin and causes severe aggregation of the off-pathway intermediate during apoflavodoxin folding. *J. Biol. Chem.* **283**, 27383–27394
39. Nabuurs, S. M., Westphal, A. H., aan den Toorn, M., Lindhoud, S., and van Mierlo, C. P. (2009) Topological switching between an α - β parallel protein

Molten Globule Formation on the Ribosome

and a remarkably helical molten globule. *J. Am. Chem. Soc.* **131**, 8290–8295

40. Nabuurs, S. M., and van Mierlo, C. P. (2010) Interrupted hydrogen/deuterium exchange reveals the stable core of the remarkably helical molten globule of α - β parallel protein flavodoxin. *J. Biol. Chem.* **285**, 4165–4172
41. Bollen, Y. J., Nabuurs, S. M., van Berkel, W. J., and van Mierlo, C. P. (2005) Last in, first out. The role of cofactor binding in flavodoxin folding. *J. Biol. Chem.* **280**, 7836–7844
42. Edmondson, D. E., and Tollin, G. (1971) Flavin-protein interactions and the redox properties of the Shethna flavoprotein. *Biochemistry* **10**, 133–145
43. Taylor, M. F., Boylan, M. H., and Edmondson, D. E. (1990) *Azotobacter vinelandii* flavodoxin: purification and properties of the recombinant, dephospho form expressed in *Escherichia coli*. *Biochemistry* **29**, 6911–6918
44. Houwman, J. A., Westphal, A. H., van Berkel, W. J., and van Mierlo, C. P. (2015) Stalled flavodoxin binds its cofactor while fully exposed outside the ribosome. *Biochim. Biophys. Acta* **1854**, 1317–1324
45. Bollen, Y. J., Westphal, A. H., Lindhoud, S., van Berkel, W. J., and van Mierlo, C. P. (2012) Distant residues mediate picomolar binding affinity of a protein cofactor. *Nat. Commun.* **3**, 1010
46. Nakatogawa, H., and Ito, K. (2002) The ribosomal exit tunnel functions as a discriminating gate. *Cell* **108**, 629–636
47. Schaffitzel, C., and Ban, N. (2007) Generation of ribosome nascent chain complexes for structural and functional studies. *J. Struct. Biol.* **158**, 463–471
48. Timasheff, S. N., and Arakawa, T. (1989) in *Stabilization of Protein Structure by Solvents* (Creighton, T. E., ed) pp. 331–345, IRL Press, Oxford, UK
49. Steensma, E., Heering, H. A., Hagen, W. R., and Van Mierlo, C. P. (1996) Redox properties of wild-type, Cys69Ala, and Cys69Ser *Azotobacter vinelandii* flavodoxin II as measured by cyclic voltammetry and EPR spectroscopy. *Eur. J. Biochem.* **235**, 167–172
50. van Mierlo, C. P., van Dongen, W. M., Vergeldt, F., van Berkel, W. J., and Steensma, E. (1998) The equilibrium unfolding of *Azotobacter vinelandii* apoflavodoxin II occurs via a relatively stable folding intermediate. *Protein Sci.* **7**, 2331–2344
51. Lindhoud, S., van den Berg, W. A., van den Heuvel, R. H., Heck, A. J., van Mierlo, C. P., and van Berkel, W. J. (2012) Cofactor binding protects flavodoxin against oxidative stress. *PLoS One* **7**, e41363
52. Steensma, E., and van Mierlo, C. P. (1998) Structural characterisation of apoflavodoxin shows that the location of the stable nucleus differs among proteins with a flavodoxin-like topology. *J. Mol. Biol.* **282**, 653–666
53. Cymer, F., Hedman, R., Ismail, N., and von Heijne, G. (2015) Exploration of the arrest peptide sequence space reveals arrest-enhanced variants. *J. Biol. Chem.* **290**, 10208–10215
54. Goldman, D. H., Kaiser, C. M., Milin, A., Righini, M., Tinoco, I., Jr., and Bustamante, C. (2015) Ribosome. Mechanical force releases nascent chain-mediated ribosome arrest *in vitro* and *in vivo*. *Science* **348**, 457–460
55. Ban, N., Nissen, P., Hansen, J., Moore, P. B., and Steitz, T. A. (2000) The complete atomic structure of the large ribosomal subunit at 2.4 Å resolution. *Science* **289**, 905–920
56. Eichmann, C., Preissler, S., Riek, R., and Deuerling, E. (2010) Cotranslational structure acquisition of nascent polypeptides monitored by NMR spectroscopy. *Proc. Natl. Acad. Sci. U.S.A.* **107**, 9111–9116
57. Ellis, J. P., Culviner, P. H., and Cavagnero, S. (2009) Confined dynamics of a ribosome-bound nascent globin: Cone angle analysis of fluorescence depolarization decays in the presence of two local motions. *Protein Sci.* **18**, 2003–2015
58. Kaiser, C. M., Goldman, D. H., Chodera, J. D., Tinoco, I., Jr., and Bustamante, C. (2011) The ribosome modulates nascent protein folding. *Science* **334**, 1723–1727
59. Klugkist, J., Voorberg, J., Haaker, H., and Veeger, C. (1986) Characterization of three different flavodoxins from *Azotobacter vinelandii*. *Eur. J. Biochem.* **155**, 33–40
60. Wang, M., Roberts, D. L., Paschke, R., Shea, T. M., Masters, B. S., and Kim, J. J. (1997) Three-dimensional structure of NADPH-cytochrome P450 reductase: Prototype for FMN- and FAD-containing enzymes. *Proc. Natl. Acad. Sci. U.S.A.* **94**, 8411–8416
61. Garcin, E. D., Bruns, C. M., Lloyd, S. J., Hosfield, D. J., Tiso, M., Gachhui, R., Stuehr, D. J., Tainer, J. A., and Getzoff, E. D. (2004) Structural basis for isozyme-specific regulation of electron transfer in nitric-oxide synthase. *J. Biol. Chem.* **279**, 37918–37927

The Ribosome Restrains Molten Globule Formation in Stalled Nascent Flavodoxin
Joseline A. Houwman, Estelle André, Adrie H. Westphal, Willem J. H. van Berkel and
Carlo P. M. van Mierlo

J. Biol. Chem. 2016, 291:25911-25920.
doi: 10.1074/jbc.M116.756205 originally published online October 26, 2016

Access the most updated version of this article at doi: [10.1074/jbc.M116.756205](https://doi.org/10.1074/jbc.M116.756205)

Alerts:

- [When this article is cited](#)
- [When a correction for this article is posted](#)

[Click here](#) to choose from all of JBC's e-mail alerts

This article cites 60 references, 16 of which can be accessed free at
<http://www.jbc.org/content/291/50/25911.full.html#ref-list-1>